J Fluoresc (2010) 20:19–26
DOI 10.1007/s10895-009-0517-4

ORIGINAL PAPER

Elucidating Anomalous Protein Diffusion in Living Cells with Fluorescence Correlation Spectroscopy—Facts and Pitfalls

Nina Malchus · Matthias Weiss

Received: 11 May 2009 / Accepted: 29 June 2009 / Published online: 7 July 2009

Abstract Anomalous protein diffusion has been frequently observed in intracellular fluids and on membranes of living cells. Indeed, a large variety of specimen, from bacteriae to mammalian cells, and several non-invasive measurement techniques, e.g. fluorescence correlation spectroscopy, have revealed that the mean square displacement (MSD) of proteins in vivo is often characterized by an anomalous power-law increase $\langle r(t)^2 \rangle \sim t^\alpha$ with $0.5 < \alpha \leq 0.8$. Here, we review these results with a particular focus on fluorescence correlation spectroscopy, and we report on possible causes of variations of the anomaly degree α. Moreover, we highlight generic consequences of anomalous diffusion that are likely to play an important role in the cellular context.

Keywords Anomalous diffusion · Fluorescence correlation spectroscopy · Macromolecular crowding · Membranes

Introduction

Diffusion is the basic mode of motion in living cells. In contrast to the energy-consuming long-distance transport via molecular motors on cytoskeletal elements, thermally driven diffusion is responsible for the short-scale movement of molecules. Diffusion is therefore essential to establish protein–protein interactions locally, e.g. in the context of cellular signaling cascades.

Besides the knowledge about the time scale needed for diffusive transport, measuring the diffusion coefficient also reveals important additional information: Via the size dependence of the diffusion constant D one may determine if a protein is in complex with other macromolecules, while the dependence of D on the surrounding fluid's viscosity yields valuable information about the protein's environment. Diffusion therefore probes the local material properties of intracellular fluids.

At first glance one may expect the intracellular environment of living cells to be a homogenous and aqueous fluid in which proteins are dissolved. Indeed, standard biochemistry often relies on this assumption, i.e. fairly dilute, aqueous solutions are typically used for in vitro protein assays. However, when inspecting the cell more closely, the picture needs to be updated. The cytoplasm of living cells is highly crowded with a plethora of proteins and other macromolecules, reaching a total concentration of up to 400 mg/ml [7]. This degree of crowding may even raise concerns as to whether one may speak of the existence of free water molecule in the cell or if one rather has to view all water molecules as being part of very thin hydration shells around proteins and membranes.

The crowding situation is similar on membranes, where already the surface density of transmembrane

N. Malchus · M. Weiss (✉)
Cellular Biophysics Group,
German Cancer Research Center,
c/o BIOQUANT, Im Neuenheimer Feld 267,
69120 Heidelberg, Germany
e-mail: m.weiss@dkfz.de

proteins is extremely high ($3 \times 10^4/\mu m^2$) [14, 27]. Taking also peripheral membrane proteins into account, cellular membranes are indeed as crowded as the cytoplasm and nucleoplasm.

The mere excluded volume in crowded environments already gives rise to a series of remarkable phenomena like enhanced complex formation and protein folding (see, e.g., [25] for a comprehensive review). On the other hand, it is easy to imagine that thermally driven motion, i.e. diffusion of single proteins, may be qualitatively and quantitatively different from the Brownian motion in dilute environments. In this review, we will focus on the anomalous diffusion behavior of macromolecules in crowded intracellular environments, i.e. in intracellular fluids and on cellular membranes. We will put a particular emphasis on how to assess this phenomenon with fluorescence correlation spectroscopy (FCS) and which pitfalls may be expected in the evaluation of FCS data.

Anomalous diffusion: where, when, and why?

Several techniques, e.g. fluorescence correlation spectroscopy (FCS), single particle tracking (SPT), and fluorescence recovery after photobleaching (FRAP) have been used to uncover anomalous diffusion of macromolecules in the cytoplasm of bacteria [8, 13] and yeast [39], and in the cytoplasm [16, 17, 44] and nucleoplasm [16, 17, 41] of mammalian cells. In line with these findings, anomalous diffusion was also observed in crowded protein solutions [1, 16, 17, 45]. Anomalous diffusion of membrane proteins and lipids has been observed on the plasma membrane [30, 38], on intracellular membranes [43], and on artificial membranes [36, 37].

Common to all of these experimental observations is a nonlinear scaling of the mean square displacement (MSD) with time, i.e. $\langle r(t) \rangle \sim t^\alpha$ with $\alpha < 1$ ($\alpha = 1$ for normal diffusion). Anomalous diffusion with $\alpha < 1$ is often referred to as 'subdiffusion'.

It is worthwhile noting already at this point that the anomalous scaling of the MSD is typically not an asymptotic behavior, but in virtually all cases represents a (long-lasting) transient that may extend over several orders of magnitude in time. Therefore, various experimental techniques, probing different length and time scales, may highlight the normal or anomalous scaling regimes of the MSD.

In fact, subdiffusion can arise due to a variety of reasons [4, 24], e.g. due to obstruction of the random walk [4] or due to binding to immobile traps [32]. In the first scenario, a protein diffuses in a maze of (immobile) obstacles and its diffusion becomes anomalous when the density of obstacles approaches a critical concentration c_{perc}, the so-called percolation threshold [34]. Indeed, Monte Carlo simulations have highlighted that an obstructed random walk significantly alters experimental observables like FRAP curves [33]. In the trapping scenario, particles bind to traps with varying energy depths and are hence immobilized for varying periods of time. Mathematically, such a random walk can be reduced to a continuous time random walk (CTRW) [24], in which the diffusing particle takes power-law distributed rests between periods of free Brownian motion. The latter type of motion is particularly interesting as it shows ageing and weak ergodicity breaking [18, 21], i.e. the time-averaged MSD (used, for example, in SPT) and the ensemble-averaged MSD (used, for example, in FRAP) deviate from each other.

These caveats on length and time scales of subdiffusion in comparison to the experimentally accessible scales (using FCS, FRAP, or SPT), but also technical constraints like fitting experimental data (see next section) may be key to the interpretation of experiments that have reported normal instead of anomalous diffusion in intracellular fluids [6] or on membranes [5]. For SPT, it has also been shown that anomalous diffusion of membrane proteins can easily be missed if inadequate video rates are used [31].

Detecting anomalous diffusion by FCS

Fluorescence correlation spectroscopy (FCS) was introduced in 1972 [23], but only became a versatile tool with the advent of confocal microscopy [26, 29]. In contrast to other microscopy techniques like FRAP, FCS does not rely on the average fluorescence but rather exploits the fluorescence fluctuations. These fluctuations arise due to the motion of fluorescent molecules into and out of the confocal volume. This movement is most often a diffusion process but also directed motion can be studied with FCS [20]. Subtracting the (temporally averaged) mean fluorescence $\langle F \rangle$ from the fluorescence time series $F(t)$, one is left with the fluctuations $\delta F(t) = F(t) - \langle F \rangle$. Calculating the autocorrelation function of the fluctuations

$$C(\tau) = \frac{\langle \delta F(t) \delta F(t+\tau) \rangle}{\langle F \rangle^2} \quad (1)$$

yields a curve that decays sigmoidally in a semi-logarithmic plot (cf. Fig. 1).

In essence, the value of the autocorrelation function for a given time lag τ will depend on the similarity of the shifted and unshifted fluorescence signals, $F(t)$ and $F(t+\tau)$. For $\tau \to 0$, $C(\tau)$ has a maximum since the fluorescence values at times t and $t+\tau$ converge to the same value. In general, for lag times τ that are smaller than the typical residence time τ_D of a fluorophore in the confocal volume, the fluctuations $\delta F(t)$ and $\delta F(t+\tau)$ are positively correlated since the fluorescence values $F(t)$ and $F(t+\tau)$ arise from the same set of fluorophores that only assume different spatial configurations in the confocal volume. In the inverse limit, $\tau \gg \tau_D$, the fluctuations arise due to completely different fluorophores, i.e. there is no correlation between the fluorescence values, and consequently $C(\tau) = 0$. It is therefore possible to extract the particles' mean dwell time τ_D in the confocal volume from the sigmoidal decay of $C(\tau)$. Knowing the typical extension r_0 of the confocal volume one can derive from that (without doing any more algebra) an estimate for a diffusion coefficient via the ratio r_0^2/τ_D.

Indeed, assuming a Gaussian confocal volume and a (sub)diffusive motion of the particles, it is possible to derive the analytical form of the autocorrelation function (rigorous for $\alpha = 1$ [28], more heuristically for $\alpha < 1$ [44]):

$$C(\tau) = \frac{A}{(1+(\tau/\tau_D)^{\alpha})\sqrt{1+(\frac{\tau}{\tau_D S^{2/\alpha}})^{\alpha}}} \,. \tag{2}$$

Here, α denotes the anomaly degree of the diffusion while τ_D is the mean dwell time of a particle in the confocal volume with beam waist r_0 ($\tau_D = r_0^2/(4D)$ for $\alpha = 1$ with the diffusion constant D). The elongation of the confocal volume along the optical axis is taken into account by the structure factor S. The prefactor A is inversely proportional to the number N of particles in the confocal volume and also includes the photophysics of the fluorophore [28]. For a general and comprehensive introduction to FCS, we would like to refer the reader to [28].

Indeed, FCS in conjunction with the above fitting function has been used by various groups to study anomalous diffusion in living cells [16, 17, 41, 44] and artificially crowded fluids [1, 16, 17]. It is worthwhile noting, however, that the derivation of Eq. 2 assumes a time-dependent diffusion coefficient for $\alpha < 1$. More complicated, but mathematically sound expressions can be derived when assuming that the particles are subject to particular types of subdiffusive motion, e.g. fractional Brownian motion or a CTRW [22].

Extracting quantitative information on τ_D and α from FCS curves crucially depends on the fitting of experimental data. The same holds true, of course, for SPT and FRAP. Employing an analytical expression for the case of several diffusing, but non-interacting species [28] may even result in a fit to the experimental data which is similarly good as using Eq. 2 with anomalous diffusion (cf. [43] for discussion). The choice of the fitting function thus is of major importance for the subsequent interpretation of the data. Besides a discrimination of models via the goodness-of-fit, additional theoretical constraints are here often helpful. On membranes, for example, lipids can be regarded as the most mobile entities, i.e. the diffusion constant of membrane proteins should typically not exceed a value of about 1 $\mu m^2/s$. For the diffusion of soluble proteins, the mass implies a hydrodynamic radius from which one can estimate the diffusion coefficient, bearing in mind that intracellular fluids have a three- to fivefold higher viscosity than water [9]. For anomalous diffusion, theoretical predictions from percolation theory yield an estimate $\alpha > 0.5$ in bulk and $\alpha > 0.7$ on membranes [4]. Moreover, if the diffusive decay of the autocorrelation curve is so fast that it overlaps with the putative photophysics, determining the anomaly may

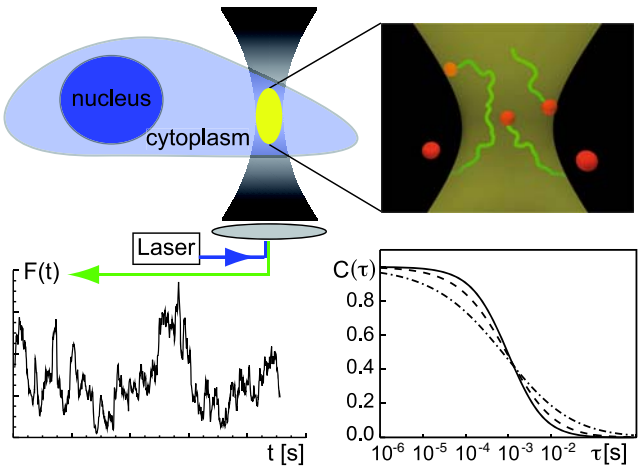

Fig. 1 Sketch of an FCS experiment in a living cell where the laser focus is parked at an intracellular locus of interest, e.g. in the cytoplasm. Fluorescent molecules diffuse into and out of the confocal volume, giving rise to fluctuations in the fluorescence time series $F(t)$. The autocorrelation function of the fluctuations, $C(\tau)$, shows a sigmoid decay on a semi-logarithmic time scale. The half-time of the decay denotes the mean dwell time of the particles in the focus. The more anomalous the diffusion of the fluorescent particles is, the more shallow is the decay of $C(\tau)$ ($\alpha = 1.0, 0.75, 0.5$ are shown as *full*, *dashed*, and *dash-dotted lines*, respectively)

become cumbersome and the use of Eq. 2 may not yield reliable results. Considering constraints like these are often extremely valuable to decide between competing fitting functions.

Sources of apparent variability of the anomaly degree

Having seen that FCS can quantitatively determine anomalous diffusion characteristics of molecules in living matter, one may ask to which extent the anomaly degree α is a well-defined quantity. Clearly, fitting and the fitting range are issues that always need a careful consideration (see above). In addition, various factors of the experimental setup and the geometry of the sample can influence the outcome of an FCS experiment [10]. Optical distortions, for example, can lead to the occurrence of an artificial, yet weak subdiffusion [19]. Also geometry effects can play a role, e.g. when FCS measurements are performed in the vicinity of a fluctuating membrane [11] or when measuring in confined volumes such as dendrites [12].

Another type of geometrical constraint is imposed by the motion of a membrane through the confocal volume, e.g. when the cytoskeleton pushes on the plasma membrane. While a static curvature of membranes does not induce subdiffusion per se [43], the membrane movement may influence the apparent anomaly degree that may be induced via crowding on the membrane. Moreover, one may ask whether a slight bleaching during the FCS experiment is responsible for the emergence and spread of anomaly degrees $\alpha < 1$.

Figure 2 depicts representative FCS curves of two membrane proteins on the plasma membrane of HeLa cells: (a) the peripheral membrane protein glycosylphosphatidylinositol-GFP (GPI-GFP) [46], and (b) the transmembrane cargo protein GFP-tsO-45-G (VSVG-GFP) [40]. Both constructs show subdiffusion with a considerable variation of the anomaly, $0.55 < \alpha < 1.2$ (cf. the distributions $p(\alpha)$ in Fig. 2c, d).

To test whether bleaching may account for the broad distribution $p(\alpha)$, we used Monte Carlo simulations of obstructed diffusion in two dimensions (see "Materials and methods" for details). To obtain a mean anomaly $\langle\alpha\rangle \approx 0.8$ that is consistent with the experimental observation, we fixed the obstacle concentration to 37%. As a result, we observed for vanishing and small bleaching rates only a minor spread of the distribution of anomalies, $p(\alpha)$ (Fig. 3a). Hence, the different configuration of obstacles (e.g. in an ensemble of cells or at different loci on the plasma membrane) cannot account for the experimentally observed variation of α.

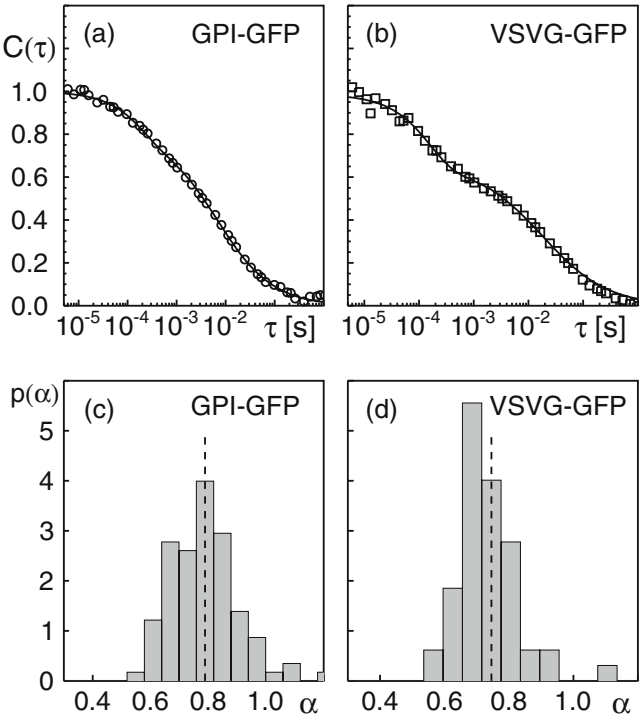

Fig. 2 Representative FCS curves for **a** GPI-GFP and **b** VSVG-GFP. Both show a subdiffusive decay behavior with $\alpha \approx 0.77$ and $\alpha \approx 0.74$, respectively. Experimental data are represented by symbols, best fits according to Eq. 3 by *full lines*. While VSVG-GFP showed a very strong triplet contribution on short time scales, GPI-GFP was less affected by the photophysics. **c, d** The distributions of anomalies $p(\alpha)$ for GPI-GFP and VSVG-GFP have a similar mean (*dashed line*) and both show a considerable variation around the mean

For higher bleaching rates the entire distribution $p(\alpha)$ shifted towards larger α yet did not significantly change its shape. Thus, the experimentally observed subdiffusion is not an artifact of bleaching since it rather increases the apparent α. Furthermore, bleaching did not increase the width of the distribution of $p(\alpha)$. It is worthwhile noting at this point that the imposed bleaching conditions did not yield a significant drop of the fluorescence in time, while the autocorrelation curve was altered. Since bleaching adds another means to destroy the temporal correlations of the fluorescence, the steeper decay behavior is well anticipated. The observation that the mean anomaly $\langle\alpha\rangle$ but not the shape of $p(\alpha)$ changes upon bleaching may yield yet another explanation why some FCS studies observed normal diffusion in crowded media and in the cellular context.

We next examined the distribution $p(\alpha)$ when the membrane substrate is moving. Besides the thermal undulations of membranes, also active processes within the cell (mediated, for example, via the cytoskeleton)

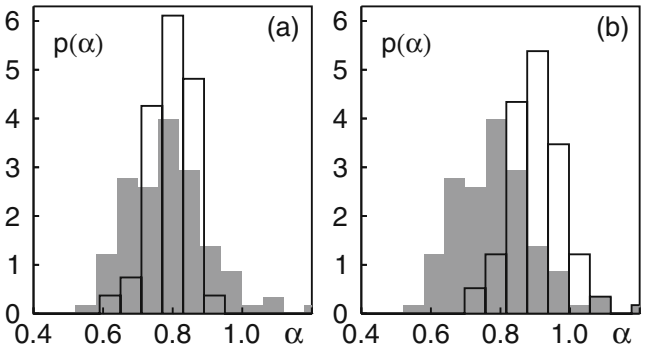

Fig. 3 **a** Distribution of anomalies $p(\alpha)$ obtained from simulations (*black line histogram*) for obstructed diffusion using an obstacle density 37% but different random configurations of the obstacles. The width of $p(\alpha)$ is smaller than the experimentally observed one for GPI-GFP (*grey-shaded*). **b** Same as in (**a**) but with an additional bleaching inside the FCS focus. While small bleaching rates had no effect, a moderate bleaching (rate $r = 10/\mathrm{s}$) shifted $p(\alpha)$ towards larger anomalies (*black line histogram*), i.e. the motion appeared more like normal diffusion. The experimentally observed distribution for GPI-GFP is shown *grey-shaded*

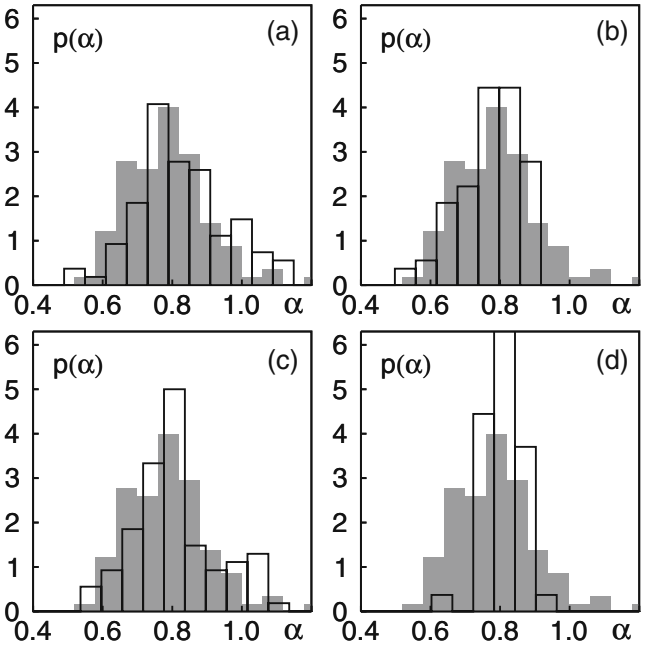

Fig. 4 **a** Distribution of anomalies $p(\alpha)$ obtained from simulations for obstructed diffusion (obstacle density 37%, random configurations) when the plane in which the particles performed the random walk moved diffusively along the optical axis of the imposed FCS focus. An enhanced up-and-down movement (max. excursion 2 μm) yielded a distribution $p(\alpha)$ (*black line histogram*) that was similar to the experimentally observed one for GPI-GFP (*grey-shaded*). **b** Restricting the excursions of the plane to 800 nm or less revealed considerable deviations from the experimental data for large α. **c** Tilting the plane diffusively (60° maximum angle) with respect to the optical axis of the imposed FCS focus yielded a distribution $p(\alpha)$ (*black line histogram*) that was very similar to the experimentally observed one for GPI-GFP (*grey-shaded*). **d** Restricting the tilt angle to 20° or less, strong deviations with respect to the experimental data (*grey-shaded*) are visible

may rock and move the plasma membrane. We therefore mimicked the membrane dynamics by an up-and-down movement and tilting of the simulation plane with respect to the optical axis. Again, we chose a constant obstacle concentration (37%) and varied the obstacle configuration for each simulation. In each time step the tilt angle θ between the optical axis and the membrane normal or the position along the optical axis was varied stochastically in addition to the in-plane (sub)diffusion of the tracer particles.

Taking an ensemble average over different maximal amplitudes and different maximal step sizes per time step, we observed a broading of $p(\alpha)$ when large excursion and tilt amplitudes (Fig. 4) were allowed. Restricting the membrane dynamics to smaller tilt angles or up-and down excursions showed a considerable decrease in the width of the anomaly distribution.

Our simulation results show that the membrane dynamics and also bleaching can significantly affect the apparent anomaly of a molecule's random walk. Since both perturbations directly affect the apparent propagator of the fluorescent particles (the central quantity that is determined via FCS, FRAP and SPT) the described uncertainties are not a mere property of FCS, but rather affect all available fluorescence techniques.

Last but not least we also would like to comment on the variability of α in bulk experiments, e.g. when performing FCS in the cytoplasm. Due to the heterogeneity of these crowded and complex fluids, a spread in $p(\alpha)$ is well anticipated. Yet, despite the contribution of nearby surfaces (membranes of larger organelles), FCS experiments in bulk are less sensitive than on membranes. For crowded protein solutions one finds even a width of $p(\alpha)$ that is consistent with the above simulations on obstructed random walks with a fixed obstacle density but different obstacle configurations (cf. Fig. 3). Hence, it appears fair to say that α is somewhat better defined in bulk experiments while measurements on membranes require an extensive statistics to determine at least the mean anomaly $\langle\alpha\rangle$ of the random walk.

What are consequences of anomalous diffusion?

The occurrence of anomalous diffusion raises the immediate question for possible consequences on the secret life of a cell. Indeed, simulation studies have highlighted a number of possibilities. On one hand, the amount of products may increase if the reaction rate is

quite low [35] since subdiffusion considerably increases the residence time of two reactants in the interaction range. Also, the kinetics of enzymatic reactions, i.e. the usual Michaelis–Menten scheme, shows fractional behavior [3]. It has also been shown, that the formation of Turing patterns that are often implicated in patterning processes in developmental biology, is significantly enhanced when one of the reagents is subdiffusive [42].

In addition, a very general phenomenon has recently been put forward. Assuming that a protein searches an (immobile) target via (sub)diffusion, one may ask for the probability $P(R)$ of getting captured when starting the search at a distance R from the target. This diffuse-to-capture scenario has been repetitively used in soft-condensed matter and biophysics. Indeed, an easy scaling relation is found in the case of normal diffusion: $P(R) \sim 1/R$ [2]. Strikingly, subdiffusion can outperform this capture probability if the search is given enough time [15]. In better words, subdiffusion yields a much higher capture probability as compared to normal diffusion, thereby rendering subdiffusion the more extensive search algorithm. The basic reason for this surprising behavior is the fractal dimension of the search path that is plane-filling but not bulk-filling for normal diffusion. Subdiffusion, however, can become even bulk-filling due to its non-Brownian random walk.

In summary, subdiffusion appears to occur naturally in all living organisms, in intracellular fluids and on membranes, and it has great implications on the dynamics of biological processes.

Materials and methods

Cell culture and microscopy

HeLa cells were cultured and prepared for microscopy as described before [16]. Transfection was performed using FuGene6 (Roche) and the manufacturer's protocol using the plasmids for VSVG-GFP [40] and GPI-GFP [46].

Imaging and fluorescence correlation spectroscopy (FCS) was performed with a Leica SP2-TCS confocal laser scanning microscope equipped with a water immersion objective (HCX PL APO 63x1.2W CORR) and an FCS-unit (Leica Microsystems, Mannheim, Germany). Samples were illuminated using the 488nm line of an Argon laser; fluorescence was detected using a bandpass filter (500–530 nm). The pinhole was set to one Airy unit. Microscope and sample were kept at constant temperature (37 °C) by a climate chamber (Life Imaging Services, Reinach, Switzerland). For the measurement, cells were supplied with MEM (without phenol red) and 25 mM Hepes. The focus was set on the plasma membrane parallel to the coverslip, at the position with the maximum intensity. In total, 96 and 54 curves were collected in different cells over various days for GPI-GFP and VSVG-GFP, respectively. The day to day variability was not larger than the variability of measurements recorded the same day. Data acquisition times were 20–50 s.

FCS data were fitted with an appropriate mathematical expression for (anomalous) diffusion on a two-dimensional substrate [28, 43]:

$$C(\tau) = \frac{(1 + f_T \exp(-\tau/\tau_T))/N}{1 + (\tau/\tau_D)^{\alpha}} \,. \tag{3}$$

Here, α denotes the degree of anomaly of the diffusion while τ_D is the mean dwell time of a particle in the confocal volume (for $\alpha = 1$ this yields the diffusion coefficient via $\tau_D = r_0^2/(4D)$ with the beam waist r_0). The mean number of particles in the confocal volume is denoted by N, whereas f_T denotes the fraction of fluorophores in the triplet state having a lifetime τ_T. VSVG-GFP showed a pronounced photophysics due to the particular GFP variant [40]. Only FCS curves that yielded a stable and unambiguous fit were considered.

Simulations

The (anomalous) diffusion of a membrane protein was simulated by (obstructed) diffusion on a square lattice using periodic boundary conditions and the blind ant algorithm. To achieve a subdiffusive behavior, we randomly placed immobile obstacles on 37% of the lattice sites (see main text for specific values). These values are near to the percolation threshold and thus show a transient subdiffusion with an anomaly $\alpha > 0.7$ [4]. Free particles ($N = 500$) were assumed to have a diffusion constant $D = 2\ \mu\text{m}^2/\text{s}$. The lattice size was 3.5 μm × 3.5 μm with a lattice constant of $\Delta x = 10$ nm (i.e. 350 × 350 lattice sites). The time increment was $\Delta t = 10$ μs.

To obtain FCS curves, a Gaussian confocal volume of width $\sigma_x = \sigma_y = 250$ nm and $\sigma_z = 5\sigma_x$ was placed in the center of the lattice and particles were assumed to contribute to the total fluorescence proportional to the Gaussian value on their lattice site. To avoid finite-size effects, the lattice was chosen 14-fold larger than r_0. Before data acquisition, 10^6 equilibration steps were performed. Data were recorded for 20 s, comparable to the experimental data acquisition time.

Initially, the lattice was taken to be perpendicular to the optical axis in the center of the confocal volume. To mimic membrane undulations, an erratic motion along, or a dynamic tilting of the lattice with respect to the optical axis was imposed. Movement up and down along the optical axis was modeled as a random walk with a diffusion constant D_z in a harmonic potential (spring constant k_z). We have chosen 9 different combinations of values for these two parameters to mimic membrane undulations of varying strength, namely $D_z = 0.3, 3, 30\ \mu m^2/s$ which corresponded to maximum step sizes of 1, 12, and 40 nm per time step. The strength of the harmonic potential, k_z, was adjusted for each D_z to achieve three typical excursion heights $z = 0.25\ \mu m, 0.8\ \mu m, 2\ \mu m$. Thus, three different diffusive step sizes were combined with three different maximal excursions from the focal plane. For each of these nine combinations ten runs with independent obstacle distributions were performed. The combination of these data is shown in Fig. 4a.

Similarly, tilting was a random walk in angle space with diffusion coefficient D_θ in a harmonic potential of strength k_θ. Here we have tested 6 different parameter sets: $D_\theta = 0.01, 0.1, 1\ rad^2/s$ giving rise to maximal changes of 0.05°, 0.15°, 0.5° in the angle θ per time step. For each value of D_θ the strength of the harmonic potential was adjusted to allow for maximal tilt angles of either 60° or 20°. For each of these 6 parameter sets, we simulated 10 FCS curves with random obstacle distributions. The combination of these data is shown in Fig. 4b.

Bleaching was implemented as a stochastic process with a rate that depended on the position of the particle in the imposed Gaussian focus, i.e. the bleaching rate was highest in the center of the FCS focus. This maximum bleaching rate r was varied in the range $0.1, \ldots, 10/s$. Here the number of particles was increased to $N = 2,000$ on an array of size $10 \times 10 \mu m^2$.

Acknowledgements This work was supported by the Institute for Modeling and Simulation in the Biosciences (BIOMS) in Heidelberg. NM was funded by the Harmut Hoffmann-Berling International Graduate School of Molecular and Cellular Biology, Heidelberg.

References

1. Banks DS, Fradin C (2005) Anomalous diffusion of proteins due to molecular crowding. Biophys J 89(5):2960–2971
2. Berg HC (1993) Random walks in biology. Princeton University Press, Princeton
3. Berry H (2002) Monte carlo simulations of enzyme reactions in two dimensions: fractal kinetics and spatial segregation. Biophys J 83:1891–1901
4. Boucheaud JP, Georges A (1990) Anomalous diffusion in disordered media—statistical mechanisms, models, and physical applications. Phys Rep 195:127–293
5. Crane JM, Verkman AS (2008) Long-range nonanomalous diffusion of quantum dot-labeled aquaporin-1 water channels in the cell plasma membrane. Biophys J 94:702–713
6. Dix JA, Verkman AS (2008) Crowding effects on diffusion in solutions and cells. Annu Rev Biophys 37:247–263
7. Ellis RJ, Minton AP (2003) Cell biology: join the crowd. Nature 425:27–28
8. Elowitz MB, Surette MG, Wolf PE, Stock JB, Leibler S (1999) Protein mobility in the cytoplasm of *Escherichia coli*. J Bacteriol 181:197–203
9. Elsner M, Hashimoto H, Simpson JC, Cassel D, Nilsson T, Weiss M (2003) Spatiotemporal dynamics of the COPI vesicle machinery. EMBO Rep 4:1000–1004
10. Enderlein J, Gregor I, Patra D, Fitter J (2004) Art and artefacts of fluorescence correlation spectroscopy. Curr Pharm Biotechnol 5:155–161
11. Fradin C, Abu-Arish A, Granek R, Elbaum M (2003) Fluorescence correlation spectroscopy close to a fluctuating membrane. Biophys J 84:2005–2020
12. Gennerich A, Schild D (2000) Fluorescence correlation spectroscopy in small cytosolic compartments depends critically on the diffusion model used. Biophys J 79:3294–3306
13. Golding I, Cox EC (2006) Physical nature of bacterial cytoplasm. Phys Rev Lett 96:098102
14. Griffiths G, Warren G, Quinn P, Mathieu-Costello O, Hoppeler H (1984) Density of newly synthesized plasma membrane proteins in intracellular membranes. I. Stereological studies. J Cell Biol 98:2133–2141
15. Guigas G, Weiss M (2008) Sampling the cell with anomalous diffusion—the discovery of slowness. Biophys J 94:90
16. Guigas G, Kalla C, Weiss M (2007) Probing the nano-scale viscoelasticity of intracellular fluids in living cells. Biophys J 93:316–323
17. Guigas G, Kalla C, Weiss M (2007) The degree of macromolecular crowding in the cytoplasm and nucleoplasm of mammalian cells is conserved. FEBS Lett 581:5094–5098
18. He Y, Burov S, Metzler R, Barkai E (2008) Random time-scale invariant diffusion and transport coefficients. Phys Rev Lett 101(5):058101
19. Hess ST, Webb WW (2002) Focal volume optics and experimental artifacts in confocal fluorescence correlation spectroscopy. Biophys J 83:2300–2317
20. Kohler RH, Schwille P, Webb WW, Hanson MR (2000) Active protein transport through plastid tubules: velocity quantified by fluorescence correlation spectroscopy. J Cell Sci 113:3921–3930
21. Lubelski A, Sokolov IM, Klafter J (2008) Nonergodicity mimics inhomogeneity in single particle tracking. Phys Rev Lett 100(25):250602
22. Lubelski A, Klafter J (2009) Fluorescence correlation spectroscopy: the case of subdiffusion. Biophys J 96(6):2055–2063
23. Magde D, Elson EL, Webb WW (1974) Fluorescence correlation spectroscopy. II. An experimental realization. Biopolymers 13:29–61
24. Metzler R, Klafter J (2004) The restaurant at the end of the random walk: recent developments in the description of anomalous transport by fractional dynamics. J Phys A Math Gen 37:R161–R208

25. Minton A (2006) How can biochemical reactions within cells differ from those in test tubes? J Cell Sci 119:2863–2869
26. Nie S, Chiu DT, Zare RN (1994) Probing individual molecules with confocal fluorescence microscopy. Science 266:1018–1021
27. Quinn P, Griffiths G, Warren G (1984) Density of newly synthesized plasma membrane proteins in intracellular membranes ii. biochemical studies. J Cell Biol 98:2142–2147
28. Rigler R (2001) Fluorescence correlation spectroscopy. Springer, Berlin
29. Rigler R, Mets U, Widengren J, Kask P (1993) Fluorescence correlation spectroscopy with high count rate and low background – analysis of translational diffusion. Eur Biophys J 22:169–175
30. Ritchie K, Shan XY, Kondo J, Iwasawa K, Fujiwara T, Kusumi A (2005) Detection of non-brownian diffusion in the cell membrane in single molecule tracking. Biophys J 88:2266–2277
31. Ritchie K, Shan X-Y, Kondo J, Iwasawa K, Fujiwara T, Kusumi A (2005) Detection of non-brownian diffusion in the cell membrane in single molecule tracking. Biophys J 88:2266–2277
32. Saxton MJ (2007) A biological interpretation of transient anomalous subdiffusion. I. qualitative model. Biophys J 92:1178–1191
33. Saxton MJ (2001) Anomalous subdiffusion in fluorescence photobleaching recovery: a Monte Carlo study. Biophys J 81:2226–2240
34. Saxton MJ (1994) Anomalous diffusion due to obstacles: a Monte Carlo study. Biophys J 66:394–401
35. Saxton MJ (2002) Chemically limited reactions on a percolation cluster. J Chem Phys 116:203–208
36. Schutz GJ, Schindler H, Schmidt T (1997) Single-molecule microscopy on model membranes reveals anomalous diffusion. Biophys J 73:1073–1080
37. Schwille P, Korlach J, Webb WW (1999) Fluorescence correlation spectroscopy with single-molecule sensitivity on cell and model membranes. Cytometry 36:176–182
38. Smith PR, Morrison IE, Wilson N, Fernandez KM, Cherry RJ (1999) Anomalous diffusion of major histocompatibility complex class i molecules on hela cells determined by single particle tracking. Biophys J 76:3331–3344
39. Tolic-Norrelykke IM, Munteanu EL, Thon G, Oddershede L, Berg-Sorensen K (2004) Anomalous diffusion in living yeast cells. Phys Rev Lett 93:078102
40. Toomre D, Keller P, White J, Olivo JC, Simons K (1999) Dual-color visualization of trans-Golgi network to plasma membrane traffic along microtubules in living cells. J Cell Sci 112:21–33
41. Wachsmuth M, Waldeck W, Langowski J (2000) Anomalous diffusion of fluorescent probes inside living cell nuclei investigated by spatially-resolved fluorescence correlation spectroscopy. J Mol Biol 298:677–689
42. Weiss M (2003) Stabilizing turing patterns with subdiffusion in systems with low particle numbers. Phys Rev E 68:036213.1–036213.5
43. Weiss M, Hashimoto H, Nilsson T (2003) Anomalous protein diffusion in living cells as seen by fluorescence correlation spectroscopy. Biophys J 84(6):4043–4052
44. Weiss M, Elsner M, Kartberg F, Nilsson T (2004) Anomalous subdiffusion is a measure for cytoplasmic crowding in living cells. Biophys J 87:3518–3524
45. Wong IY, Gardel ML, Reichman DR, Weeks ER, Valentine MT, Bausch AR, Weitz DA (2004) Anomalous diffusion probes microstructure dynamics of entangled f-actin networks. Phys Rev Lett 92:178101
46. Zacharias DA, Violin JD, Newton AC, Tsien RY (2002) Partitioning of lipid-modified monomeric gfps into membrane microdomains of live cells. Science 296:913–916